THE ASTROPHYSICAL JOURNAL, 419:104–110, 1993 December 10

SHARP H I EDGES IN THE OUTSKIRTS OF DISK GALAXIES

EDVIGE CORBELLI[1]
Osservatorio Astrofisico di Arcetri, Largo E. Fermi 5, 50125 Firenze, Italy
AND
EDWIN E. SALPETER[2]
Center for Radiophysics and Space Research, Cornell University, Ithaca, NY 14853
Received 1992 December 28; accepted 1993 June 18

ABSTRACT

Observations indicate that some extended outer disks have a sharp cutoff in the surface density of neutral hydrogen when this approaches the value of $\sim 2 \times 10^{19}$ cm^{-2}. In this paper we model these H I edges as places where the ratio of neutral to ionized hydrogen drops rapidly due to ionizing radiation. We use two different models for the vertical distribution of gas above the outer Galactic plane: in the first model we derive the density from the ideal gas law, while in the second model we insert a macroscopic pressure term and derive the density as for an isothermal slab. We consider two different sources of ionizing photons: external fluxes of different intensity and spectral index due to quasars, and a monochromatic UV flux due to neutrino decays inside and outside the disk. We find that galaxies which have a smaller gas scale height, because of a higher dark matter density or a larger external pressure, should show outer H I disks to a lower column density and smoother H I edges. The sharpness of the H I–H II transition and the total column density at which the medium is 50% ionized, are strongly correlated, irrespective of the gas or photon flux model used. We present several model fits to the H I sharp edge observed in the nearby galaxy M33. If today's UV background is dominated by attenuated quasar light and gives $\sim 10^{-14}$ H ionizations s^{-1}, a large gas scale height or equivalently a nearly spherical halo is preferred. If ionizing photons from decaying neutrinos are responsible for the M33 sharp edge, then a thin outer H I disk, and consequently a flat dark matter halo, is required.

Subject headings: galaxies: ISM — radio lines: galaxies

1. INTRODUCTION

The characteristics of neutral hydrogen outside the star forming regions of disk galaxies have been outlined by Corbelli & Salpeter (1993, hereafter Paper I). In particular we have focused on the heating inputs to the gas in low-pressure conditions, which favor non-LTE and make the H I spin temperature deviate strongly from the kinetic temperature of the gas. Paper I was intended for observers who have measured the H I spin temperature through 21 cm absorption lines and want to use it to derive information on the cosmic background or local nonionizing sources. In the present paper we study H I sharp edges discovered in spiral galaxies (M33, NGC 3198) and in surveys of high-velocity clouds (HVC). In outer disks the H I column density decreases slowly with radius until a sharp edge occurs at $N_{\rm HI} = N_l \sim 2 \times 10^{19}$ cm^{-2} (Corbelli, Schneider, & Salpeter 1989; van Gorkom 1991); no residual H I is detected in emission at larger radii. Similarly, surveys of HVC have shown that there is a transitional column density $N_l = 5 \times 10^{18}$ cm^{-2} such that appreciable emission is seen for $N_{\rm HI} > N_l$ but little emission is seen for 10^{18} cm$^{-2} < N_{\rm HI} < N_l$ (Colgan, Salpeter, & Terzian 1990). In Paper I we have shown that these H I edges cannot be due to subthermal effects, i.e., to a drastic depression of the 21 cm emission line when the density of the medium is lower than a critical value and the spin temperature deviates strongly from the gas kinetic temperature. Here we test a totally different possibility for H I edges, i.e., that they are H I–H II transitions due to an ionizing flux which interacts with the neutral hydrogen distribution.

The lack of star-forming regions in the outskirts of spiral galaxies makes the cosmic background radiation extremely important for H I ionization. This background is not directly observable because it is easily absorbed by the thick H I layer in the Galactic plane. A careful comparison between sensitive H I emission studies in outer regions and theoretical results on the interaction between an ionizing background and a gas layer, can give important information on the spectrum and intensity of the cosmic background below 100 eV. Several papers have discussed this method (Felten & Bergeron 1969; Sunyaev 1969; Silk & Sunyaev 1976; Bochkarev & Sunyaev 1977); however, due to the lack of reliable information on low surface brightness H I and on the mass distribution in outer regions at that time, they could not draw any conclusion on the cosmic background. We discuss the properties of H I edges, how they can change from one type of galaxy to another and from one type of object to another (from outer disks to HVC, for example). In this paper we focus on models which can reproduce the characteristics of the edge which has been observed with good sensitivity in M33.

Details on the cosmic background radiation, on the equilibrium equations and parameters used for the gas distribution are described in § 2. In § 3 we give some scaling relation for the gas distribution around H I edges and in § 4 we derive numerical results for H I edges due to several background models and give fits to the M33 sharp edge. The characteristics of H I edges in outer disks which have local ionizing photons from the decay of dark matter are examined in § 5. We summarize and

[1] E-mail: edvige@arcetri.astro.it.
[2] E-mail: hann@astrosun.tn.cornell.edu.

discuss our results for the cosmic UV background and the gas distribution in the outskirts of disk galaxies in § 6.

2. EQUILIBRIUM MODELS FOR THE GAS IN OUTER REGIONS

The ionization-recombination equilibrium depends on the photon spectrum and on the gas density distribution. The UV and soft X-ray background has been reviewed in Paper I. For the purpose of this paper, however, the spectrum above 0.5 keV is not relevant because we are mainly interested in the ionizing effect of the cosmic radiation, and photons with energy close to the Lyman limit are the most important. As in Paper I we use the following spectral form with two parameters for the extragalactic spectrum between 13.6 and 500 eV:

$$\frac{dN}{dE} = IE_{\rm keV}^{-s} \text{ photons cm}^{-2}\text{ s}^{-1}\text{ sr}^{-1}\text{ keV}^{-1}\,. \qquad (1)$$

We shall mostly use a steep spectrum below 500 eV, usually $s \geq 1.4$. For $s = 1.4$ and $I \simeq 7.7$, equation (1) gives the spectral law observed above 2 keV. A background dominated by quasar light has a spectral index $s \simeq 2$–3 at zero redshift. A constraint to the extragalactic flux comes from Hα measurements in our Galaxy from which one can estimate the sum of the extragalactic and local ionizing radiation (Kutyrev & Reynolds 1989; Songalia, Bryant, & Cowie 1989). Measurements toward HVC give the conservative upper limit of 2×10^5 photons cm^{-2} s^{-1}. The spectrum suggested by Sargent et al. (1979) for the extragalactic flux ($I \simeq 15$ and $s = 2.4$) gives about 5×10^4 photons cm^{-2} s^{-1} and $\zeta \simeq 10^{-13}$ s^{-1} for the total number of ionizations per second for an unshielded neutral H atom (see Paper I, § 3). This is much lower than the value $\zeta \simeq 2.7 \times 10^{-12}$ s^{-1} obtained from an analysis of the proximity effect (Bajtlik, Duncan, & Ostriker 1988) at redshifts of about 2 and fits within some evolutionary studies of Lyman-α clouds (Ikeuchi & Turner 1991). However, some recent papers on flux evolution and low-redshift Lyman-α absorption lines estimate lower fluxes (Madau 1992; Charlton, Salpeter, & Hogan 1993). These models take into account the role of distant absorbers in decreasing with time the intensity of the cosmic radiation at energies close to the Lyman limit, and give $\zeta \sim 10^{-14}$ s^{-1} at present. The value $\zeta = 1.6 \times 10^{-14}$ s^{-1} corresponds to 6×10^{-24} ergs cm^{-2} s^{-1} sr^{-1} Hz^{-1} at the Lyman edge, if $I \simeq 1.4$ and $s = 2.5$ in equation (1). In the rest of this paper we will refer to this spectrum as the "Madau flux."

The gas is considered distributed in a slab (with the vertical extension much smaller than the horizontal one). For a given total column density, the penetrating flux, the gas kinetic temperature and $N_{\rm H\,I}/N_{\rm H\,II}$, all change with depth inside the layer. We therefore solve the radiative transfer, the first momentum and energy equations by integrating through the H I slab and iterate until the solution converges. Starting from the top of the slab we evaluate at each point the attenuation and the mean energy of the flux coming from both sides. We set the next step such that its optical depth, at this mean energy, is 0.05 normal to the plane. We use the ionization equilibrium and energy equations (eq. [8] and eq. [11] of Paper I) to find the equilibrium temperature T_K at each step. Because the mean energy of the radiation is close to the Lyman edge we do not include He III and assume that the fractional ionization of H I ($x_{\rm H}$) is equal to that of He I when the main photon energy is above 24 eV. The inclusion of He III, as well as the correct fractional ionization of He I, would make the H I edge slightly sharper because high energy photons would be absorbed by He II atoms and re-emitted at lower energies with a higher probability of ionizing H I atoms. However, since we will be doing a best fit to the available H I data this would only improve the chi-square value of the fit but it will not really make a difference in the selection of the best-fitting model. We use half solar abundance for metals and a helium density which is 10% the hydrogen density. We iterate on $x_{\rm H}$ and T_K at each step as well as on the whole solution in the slab until convergence is achieved.

There are no observations so far of the vertical structure of the gas in outer regions (at radial distances greater than 2 optical radii) or in external clouds. Even if detailed studies of face on galaxies give evidence of broad 21 cm line profiles in outer regions (see, for example, Dickey, Hanson, & Helou 1990) we don't know yet if the line width is determined by microscopic thermal motions or by bulk motion inside the disk. Therefore we shall consider separately two sets of models for the vertical gas distribution:

Model A.—This model assumes that at any height z above the gas midplane the gas pressure $P(z)$ is connected to the gas mass density $\rho(z)$ simply by the ideal gas law. In this model we do not include the gravity due to dark matter explicitly but we allow the pressure above the slab, $P_{\rm ext} = P(\infty)$, to be a free parameter, somewhat similar to the parameter P_0 in Paper I. For a given total hydrogen (H I + H II) column density, $N_{\rm tot}$, the vertical distribution of the gas is then determined by the first momentum equation which in the absence of flow reduces to the hydrostatic equilibrium equation:

$$\frac{\partial P(z)}{\partial z} = 4\pi G\rho(z)\int_0^z \rho(z)dz\,, \qquad (2)$$

where G is the gravitational constant. As discussed in Paper I, we expect thermal pressures in outer regions to be much smaller than in the luminous disk and we consider $1 \leq P_{\rm ext}/k \leq 100$ cm^{-3} K (k is the Boltzmann constant).

Model B.—In this model we omit the external pressure, but include explicitly the gravitational force due to dark matter and allow for a contribution to total pressure P^* from bulk motion, magnetic fields, cosmic rays, etc. We write

$$P^*(z) \equiv \rho(z)T^* \qquad (3)$$

where T^* must exceed the gas kinetic temperature $T_K(z)$. While $T_K(z)$ can vary with height and may change drastically from the cold to the warm H I phase, we make the assumption that T^* can be approximated by a constant throughout the whole slab. The ideal gas law in this case is used only to evaluate the internal microscopic pressure. The density $\rho(z)$ is continuous and related to the macroscopic pressure by the constant T^* as in equation (3). Here T^* is in units of (cm^2 s^{-2}) but sometimes we will express it in degrees K by multiplying it by $\mu m_{\rm H}/k$ (with μ then mean molecular weight). For the vertical gravity due to dark matter we use $F_z = -Kz$. The exact expression for K depends on the halo eccentricity and we present models with different values of K. If we assume corotation and choose a spherical distribution of dark matter with a power law radial density profile, at $z \ll R$ we have $K \simeq V^2/R^2$, V being the asymptotic rotational velocity. In this case the first momentum equation along z is

$$\frac{\partial\rho(z)}{\partial z} = -\rho(z)\left[\frac{K}{T^*}z + \frac{4\pi G}{T^*}\int_0^z \rho(z)dz\right]. \qquad (4)$$

In § 1 we mentioned that, beyond the first drop associated with the optical edge, the neutral atomic column density decreases smoothly and slowly as one proceeds radially

outward, until it reaches a critical value N_l and then drops very rapidly to unobservably small values (Corbelli et al. 1989; van Gorkom 1991). In Paper I we showed that this sharp outer H I edge cannot be an artifact due to subthermal effects in emission, but there are still two different possibilities. The first one is that the H I drop corresponds to a drop in the total hydrogen column density. If the gas is in stable circular orbits, $N_{\rm tot} = N_{\rm H\,I} + N_{\rm H\,II}$ can be an arbitrary function and it could in principle have had a sharp drop since the galaxy's formation. The second possibility favored here and by Maloney (1993) is that $N_{\rm tot}$ continues to drop only slowly below N_l but the ionization-recombination equilibrium results in $N_{\rm H\,I} \ll N_{\rm H\,II}$ for $N_{\rm H\,I} < N_l$. In the two following sections we analyze the effects of several extragalactic background models on the ionization structure of a gas slab and compare this with H I observations.

3. THE GAS VERTICAL THICKNESS AND ITS IONIZATION STRUCTURE

For a given extragalactic flux and total column density, $N_{\rm tot}$, the additional input parameter for Model A is the external pressure, $P_{\rm ext}$, and for Model B the constants K and T^*. We assume that these quantities decrease smoothly and slowly with increasing radial distance, so that they can be considered constant around the region where the H I edge occurs. We then compute the vertical structure of the gas slab as we vary $N_{\rm tot}$. We define the gas vertical scale height $z_{1/2}$ as the height above the midplane such that half of the total gas mass per unit area lies between $+z_{1/2}$ and $-z_{1/2}$. Similarly we define the H I scale height, $z_{\rm H\,I}$.

For Model A the scale height depends not only on the gas surface density and on the external pressure $P_{\rm ext}$, but also on the extragalactic flux, since this affects $T_K(z)$ and therefore the density stratification via the ideal gas law. In the optically thin regime, where $P_{\rm ext}$ is the dominant pressure term and the temperature of the medium is uniform to a good approximation, the scale height is $z_{1/2} = 0.5kN_{\rm tot}\,T_K/P_{\rm ext}$. For higher column densities, however, self-gravity is no longer negligible and the gas absorbs some of the extragalactic radiation. The variations of the optical depth and of the gas volume density along z makes the kinetic temperature vary with height. The slab has a nonisothermal structure with a scale height which depends strongly on the gas total column density, as well as on the spectrum of the incoming radiation. For this model $z_{\rm H\,I}$ inside the H I edge is very small. If such thin slabs are warped or multilayered, results for edges with an external ionizing flux should not be changed appreciably, but observations may only give the much thicker envelope instead of $z_{\rm H\,I}$. Close to the H I edge, $z_{\rm H\,I}$ have larger values because of the increased amount of warm hydrogen.

For Model B, if dark matter dominates over self-gravity, the gas density has a Gaussian vertical distribution and $z_{1/2} \simeq 0.68\sqrt{T^*/K}$, i.e., it does not depend on the column density $N_{\rm tot}$ but only on the ratio between the "pull down" due to dark matter and the "pull up" due to the inner macroscopic pressure. If instead self-gravity dominates, then the gas density is distributed as in an isothermal self-gravitating slab (Spitzer 1942; Ibañez & di Sigalotti 1984) and $z_{1/2} = 0.12T^*/(Gm_{\rm H}N_{\rm tot}) \simeq 10^{30}T^*/N_{\rm tot}$ cm (where $m_{\rm H}$ is the hydrogen mass in grams and we have used 0.1 as helium abundance in number with respect to hydrogen). In both cases however, the total gas for Model B has a vertical scale height which does not depend on the extragalactic flux but only on the local properties of the galaxy. The H I vertical scale height depends on the extragalactic flux but it will be a much smoother function than in Model A.

For a spherical halo which has $V/R \sim 6.7$ km s^{-1} kpc^{-1} ($K \sim 45$ km^2 s^{-2} kpc^{-2}) the ratio of dark matter to gas surface density for Model B is about $4 \times 10^{20}/N_{\rm tot}$. The density distribution along z near the H I edge is close to a Gaussian for most of the models we consider since $N_{\rm tot} \lesssim 10^{20}$ cm^{-2} and dark matter dominates over self gravity. For other models self-gravity is not completely negligible and we always include it in our numerical analysis. The observed variation of the thickness of the H I layer with radius have been derived for the Milky Way by Kulkarni, Blitz, & Heiles (1982) and most recently by Merrifield (1992). In the outermost part ($R \simeq 20$ kpc) Merrifield's measure for the observed vertical thickness, h_z, is of order 1.3 kpc and it increases beyond as $\Delta h_z \approx 0.15\Delta R$. If the H I distribution is assumed to be Gaussian, then h_z is the rms of the Gaussian distribution and $z_{\rm H\,I} \simeq 0.5h_z$. An H I edge which occurs further out, say at about 25 kpc, will have $h_z \sim 2$ kpc and $z_{\rm H\,I} \simeq 1$ kpc. A spherical halo with a rotational velocity of about 220 km s^{-1} and $z_{1/2} \sim z_{\rm H\,I}$ implies for Model B a value of $T^* \simeq 20{,}000$ K, or a dispersion of about 13 km s^{-1}. As might be expected this value for the parameter T^* is slightly larger than the gas kinetic temperature of warm H I or than the H I velocity dispersion measured in face-on galaxies (Huchtmeier & Bohnenstengel 1981; Shostak & van der Kruit 1984; Dickey et al. 1990). Since we don't know how the parameter K (which depends on halo eccentricity) and T^* vary from galaxy to galaxy, we shall consider models for a wide range of K/T^* values.

We describe the variations of $N_{\rm H\,I}$ with $N_{\rm tot}$ using the function:

$$y \equiv \log_{10}\frac{N_{\rm tot}}{N_{\rm H\,I}} \tag{5}$$

and define $N_{1/2}$ as the total column density which is half neutral and half ionized, i.e., $y(N_{1/2}) = 0.3$.

Consider first a hypothetical monochromatic flux of ionizing photons with photon energy E and ionization rate ζ impinging on a layer of total column density $N_{\rm tot}$ (a variable) and of constant hydrogen volume density n. Let N_E be that neutral hydrogen column density for which the optical depth is unity:

$$N_E \simeq \frac{1.3 \times 10^{17}}{g_{1f}}\left(\frac{E_{\rm eV}}{13.6}\right)^3 \text{ cm}^{-2}\,, \tag{6}$$

where g_{1f} is the gaunt factor for photoionization from ground level (Spitzer 1978). As in the simple "Strömgren sphere theory," we assume that the dimensionless quantity $\zeta/(\alpha_2 n)$ is large and we define a critical column density

$$N_c \equiv \frac{\zeta}{n\alpha_2} N_E \gg N_E\,, \tag{7}$$

where α_2 is the recombination coefficient excluding captures to the first level. The neutral column density $N_{\rm H\,I}$ then varies with $N_{\rm tot}$ as follows: for $N_{\rm tot} >$ (2 or 3) N_c, most of the hydrogen is neutral, shielded by an outer layer with $N_{\rm H\,II} \sim N_c$ and y is small. For $N_{\rm tot} < 0.5N_c$, on the other hand, the hydrogen is mostly ionized with

$$N_{\rm H\,I} \approx N_{\rm tot}\frac{\alpha_2 n}{\zeta} = \frac{N_{\rm tot}}{N_c} N_E\,. \tag{8}$$

To summarize this simple model: as $N_{\rm tot}$ drops from a little above N_c to a little below, $N_{\rm H\,I}/N_{\rm tot}$ drops rapidly. The larger

($\zeta/n\alpha_2$) is, the more rapid is the drop. Observed values of N_l where edges occur should then be of order of N_c.

Realistic fluxes are nonmonochromatic, and the shape of y as a function of N_{tot} depends on the shape of the photon spectrum. Large values of s in equation (1) should give results similar to that predicted by monochromatic photons at energies just above 13.6 eV; $N_{H\,I}$ predicted outside the edge will be small and unobservable with present-day 21 cm emission techniques. On the other hand for small s (flat spectrum), the variations of $y(N_{tot})$ should be more gradual, since photons of different energies have different values of N_E.

For the variation of conditions with radial distance R in a realistic disk, the density n varies as well as N_{tot}. For Model A we assume P_{ext} = constant and as N_{tot} decreases radially outward, the gas pressure P in the plane decreases at first and then remains near P_{ext}. The value of y increases between zero and a maximum constant value for small N_{tot}, $y_{max} \approx \log_{10}(\zeta/n\alpha_2)$. For Model B as N_{tot} decreases radially so does P^* and n; y continues to increase slowly for small N_{tot}. Numerical results on the sharpness of H I–H II transition are discussed in the next section.

4. NUMERICAL RESULTS USING THE EXTRAGALACTIC IONIZING FLUX

4.1. *A Series of Models*

In Table 1 we show some numerical results using Model A (A1 to A4) and Model B (B1 to B7). The attenuated quasar background described by Madau is used in examining cases with different galaxy parameters. The parameters are the external pressure P_{ext} for Model A and the dark matter density plus the dispersion T^* for Model B. As noted in the previous section. for the range of parameters of interest in Model B self-gravity hardly dominates over dark matter gravity. Therefore results depend mostly on the ratio K/T^* (and not on the two parameters separately) and we show them for three values of this ratio. For each model we give in Table 1 the value of $N_{1/2}$, $z_{1/2}$, and $z_{H\,I}$; for models where $z_{1/2}$ and $z_{H\,I}$ vary with N_{tot} they are given for $N_{tot} = N_{1/2}$.

For the models A1, A2, A3 an increase in pressure increases the mean volume density n, and consequently decreases the transition value $N_{1/2}$ (which is of the order of N_c, in eq. [7]). For a given spectrum N_E is constant and a decrease in $N_{1/2}/N_E$ makes the H I edge less sharp. If, for a given spectral shape, P and n were constant throughout the slab then results would depend only on the ratio I/P which would take the place of $\zeta/n\alpha_2$ in equation (7). In reality there is no exact scaling, since the internal pressure increase in the slab depends on P_{ext}/N_{tot}^2 (see eq. [2]); only when this ratio is large the pressure is radially constant ($P = P_{ext}$). For the Model B series at a given spectral shape we have the approximate scaling $N_{1/2} \propto \sqrt{Iz_{H\,I}}$ and $z_{H\,I} \approx (2/3)z_{1/2} \propto \sqrt{K/T^*}$. For Model A, $z_{H\,I}$ is surprisingly small for the smallest P_{ext} because given the large value of $N_{1/2}$ a small cold core forms at the center of the slab.

We also give results for different assumptions on the background: the spectral index is the same as that given by Madau but the intensity is 10 times stronger (B4) or the background has a spectral index different from $s = 2.5$. For model B5 we use a flatter spectrum which is an extrapolation down to 13.6 eV of the hard X-ray background spectrum, and for model B6 we use a steeper spectrum with $s = 4$ and a photon intensity at the Lyman edge 10 times stronger than Madau's flux. In Figure 1 we show the total and H I column density as function of the dimensionless parameter $x \equiv 20 - \log_{10} N_{tot}$ for various models listed in Table 1. Notice that Cases A1 and B1 give very similar H I edges despite the fact that they have different vertical scale heights. Furthermore the characteristics of H I edges corresponding to different spectra but to the same $N_{1/2}$ are similar. From Figure 1 we note that the H I column density where the curve $N_{H\,I}(x)$ is steepest is very small and unobservable with present techniques; for even smaller values of $N_{H\,I}$ the curve $N_{H\,I}(x)$ flattens out.

4.2. *Fitting the* H I *Edges Observed in* M33 *and in HVC*

Corbelli et al. (1989) show in their Figure 10 the second H I fall-off along the north side of the major axis of M33. For comparison with our models, the observed values of $N_{H\,I}$ should all be multiplied by an inclination factor $\cos(i)$; this factor is uncertain and we initially assume it is close to one. Omitting the very last point with large errors, we plot in Figures 2 and 3 the values of $N_{H\,I}(R)$ at the five outermost points (*filled circles*). Since the fractional change $\Delta R/R$ across these points is small, we assume that P_{ext} and K/T^* are con-

TABLE 1

H I–H II TRANSITION PARAMETERS

Model (1)	I (2)	s (3)	Galaxy Parameters (4)	log $N_{1/2}$ (cm^{-2}) (5)	$z_{1/2}$ (kpc) (6)	$z_{H\,I}$ (kpc) (7)	R_l(M33) (8)	χ^2(M33) (9)
A1	1.4	2.5	$P_{ext} = 3.$	19.8	2.7	0.8	30′	0.88
A2	1.4	2.5	$P_{ext} = 15.$	19.5	1.7	1	17	5.6
A3	1.4	2.5	$P_{ext} = 50.$	19.0	0.2	0.1	10	14.6
A4	14.	2.5	$P_{ext} = 15.$	20.1	2.7	0.5	62	0.14
B1	1.4	2.5	$K = 22.5$ $T^* = 1000$	19.8	4.5	2.7	23	2.1
B2	1.4	2.5	$K = 45.$ $T^* = 200$	19.5	1.4	1	17	4.3
B3	1.4	2.5	$K = 225.$ $T^* = 100$	19.3	0.45	0.3	13	7.9
B4	14.	2.5	$K = 45.$ $T^* = 200$	20.0	1.4	0.6	34	0.88
B5	7.7	1.4	$K = 45.$ $T^* = 200$	19.1	1.4	1.1	11	12.8
B6	0.022	4.0	$K = 45.$ $T^* = 200$	19.8	1.4	0.8	27	1.4
B7	150.	1.4	$K = 45.$ $T^* = 200$	19.8	1.4	1	19	3.2
AS1	Sciama's model		$P_{ext} = 15.$	19.5	<0.1	<0.1	19	4.0
AS2	Sciama's model		$P_{ext} = 50.$	19.0	<0.1	<0.1	10	15.2
BS1	Sciama's model		$K = 45.$ $T^* = 20$	19.8	0.45	0.2	36	1.3
BS2	Sciama's model		$K = 900.$ $T^* = 20$	19.5	0.11	<0.1	17	5.2
BS3	Sciama's model		$K = 4500.$ $T^* = 20$	19.3	<0.1	<0.1	14	7.8

NOTES.—P_{ext} is in units of cm^{-3} K, K is units of (km s^{-1} kpc^{-1})^2 and T^* is in units of (km s^{-1})^2. For the last five cases shown in the table the ionizing flux used is that computed by Sciama for neutrino decays with $E_\gamma = 14.6$ eV.

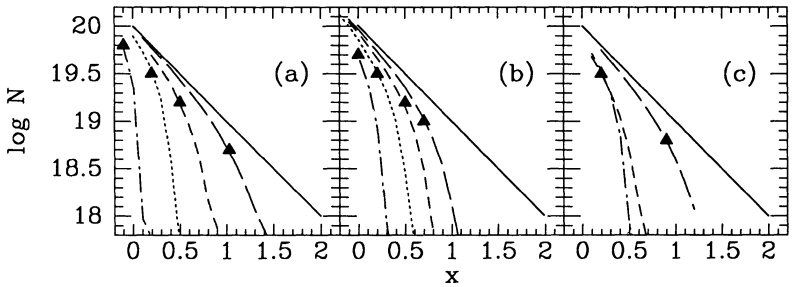

FIG. 1.—N_{tot} (*solid line*) and $N_{H\,I}$ (*dashed lines*) as functions of the dimensionless parameter $x \equiv 20 - \log_{10} N_{tot}$ for models as given in Table 1. The filled triangles indicate the H I column density at $N_{tot} = N_{1/2}$. We show cases for (*a*) Model A and (*b*) Model B. The small dashed lines refer to model A1 in (*a*) and model B1 in (*b*), the medium dashed lines refer to model A2 in (*a*) and B2 in (*b*), and the large dashed lines refer to model A3 in (*a*) and B3 in (*b*). The dot-dashed lines refer to model A4 in (*a*) and B4 in (*b*). In (*c*) the spectral slope differs from 2.5 and the models shown are B5 (*large dashed line*), B6 (*medium dashed line*) and B7 (*dot-dashed line*). B6 and B7 have the same $N_{1/2}$.

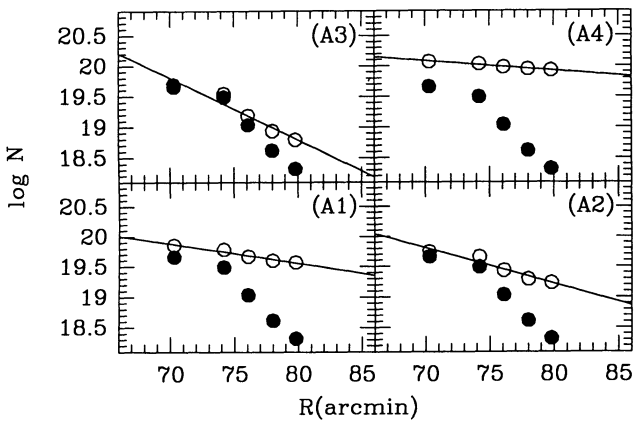

FIG. 2.—Values of $N_{H\,I}$ observed near the edge in M33 (*filled circles*) and the corresponding total gas density N_{tot} (*open circles*) for a given Model A. Models shown are labeled as in Table 1. The straight line is the best linear fit to log $N_{tot}(R)$.

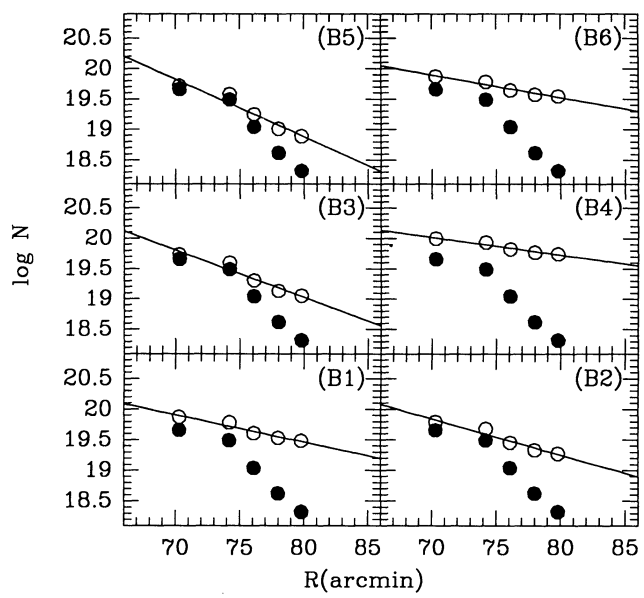

FIG. 3.—Values of $N_{H\,I}$ observed near the edge in M33 (*filled circles*) and the corresponding total gas density N_{tot} (*open circles*) for a given Model B. Six models are shown and labeled as in Table 1. The straight line is the best linear fit to log $N_{tot}(R)$.

stant across the H I fall-off. Each model listed in Table 1 gives a unique value of N_{tot} for each observed value of $N_{H\,I}$. These are shown as open circles in Figures 2 and 3. In order to compare a model with the observations we have to make some assumptions about the spatial variation of N_{tot}. We choose $N_{tot}(R) = 0.1N_0 \times 10^{R/R_l}$ and determine N_0 and the scale length R_l by a two parameter least-squares fit for each model. We fit $\log_{10} N_{tot}(R)$ assuming an rms error of ± 0.05. This is about half the error of the more rapidly varying log $N_{H\,I}$. The value of the fitted R_l and the χ^2-values for the mean squared deviations (with 3 degrees of freedom) are given in Table 1 for each model.

In the outer disk of M33 the radial fall-off of $N_{H\,I}$ changes drastically beyond 3×10^{19} cm^{-2}, suggesting that $N_c \approx N_l \simeq 2 \times 10^{19}$ cm^{-2} and $N_{1/2} \approx 4 \times 10^{19}$ cm^{-2}. Table 1 and the fits in Figures 2 and 3 show indeed that models with $N_{1/2} \lesssim 3 \times 10^{19}$ cm^{-2} give a poor fit and have large values of χ^2. They require a sudden drop in N_{tot} to fit the sharp edge, i.e., if N_{tot} is a smooth function of R they predict H I edges less sharp than observed. These models are those with large P_{ext} or K/T^* values (A3 and B3 in Figs. 2 and 3 for example) or with small ionizing backgrounds (B5 in Fig. 3). They are rather unattractive for the face-on case also because they predict very small values for R_l in M33. Although observations do not give a precise value of R_l, we know that $N_{H\,I}(R)$ before the edge occurs drops by a factor 10 in about 20 arcmin ($\approx$4 kpc, see Fig. 2 of Corbelli et al. 1989). Therefore we don't expect R_l to be much smaller than 20 arcmin for a face-on galaxy. The χ^2 improves as $N_{1/2}$ increases due to stronger ionizing fluxes or to larger gas scale heights. However, for Madau flux, values of $N_{1/2}$ larger than those shown in Table 1 require $z_{H\,I} > 5$ kpc, i.e., K noticeably smaller than estimated [K(M33) $\gtrsim 40$ km^2 s^{-2} kpc^{-2}] and unreasonably high values of T^* ($T^* > 10^3$ km^2 s^{-2}). This is to avoid self-gravity compression for these large column densities.

If the outer disk of M33 is not face-on but is inclined by an angle i, the neutral column densities perpendicular to the Galactic plane are all smaller than those observed along the line of sight. Assuming cos $i \simeq 0.7$ or 0.5 with fluxes and galaxy parameters as given in Table 1, the resulting total gas scale length, R_l, becomes larger than for a face-on disk. The χ^2 values are slightly smaller. As the galaxy gets close to be edge-on, the best value of $N_{1/2}$ decreases.

With likely values of i ($i \sim 45°$) and a spectral shape like that for quasars or steeper ($s \gtrsim 2$) good fits are obtained if intensity I and pressure are such that $N_{1/2} > N_l \simeq 2 \times 10^{19}$ cm^{-2}. For

the Madau flux, models with $P_{ext} \sim 15$ or $T^*/K \sim 4$ kpc^2 are favored since they give good fits to the sharp edge with reasonable sets of galaxy parameters for M33. For Model B a value of $T^* \sim 100$ km^2 s^{-2} (or equivalently $\sim 10^4$ K) is a lower limit since it implies $K \sim 25$ km^2 s^{-1} kpc^2, too small even for a spherical dark matter halo around M33. Slightly larger T^* and K-values are preferred. These models predict reasonable scale heights, $z_{HI} \sim 1$ or 2 kpc as observed in the outermost parts of our Galaxy (Merrifield 1992). If Merrifield's observations give evidence for an envelope of an intrinsically thinner disk with warps, vertical oscillations or multilayered slabs (clouds), then models with $z_{HI} < 1$ kpc may be more appropriate.

For HVC the shape of $N_{HI}(R)$ is unknown, but we know that N_l is smaller than in outer disks being $N_l \sim 0.5 \times 10^{19}$ cm^{-2}. A model between A2 and A3 with $P_{ext} \sim 30$ cm^{-3} K and $z_{HI} \sim 0.3$ kpc is then a possibility. Since HVC are located near the inner disk of our Galaxy, larger values of P_{ext} (due to coronal halo gas) seem reasonable. The appropriate models with smaller $N_{1/2}$ predict less sharp H I edges.

5. H I EDGES AS PREDICTED BY DARK MATTER DECAY PHOTONS

The dark matter decay theory recently developed by Sciama (Sciama 1990, 1991), predicts a universe populated by heavy neutrinos which decay radiatively producing photons with energy $E_\gamma = 13.6 + \epsilon$ with $\epsilon \sim 1$ eV and a production rate proportional to the density of dark matter. In this section we examine the possibility that sharp H I–H II transitions in outer regions are due to these low energy photons (Melott 1984) which are generated both inside and outside the gas slab. If the local density of the gas is sufficiently high (as in the optical regions of galaxies), these photons are produced and absorbed locally and they represent the most important source of photons for H I ionization. However, in considering the effects of neutrino decay in outer regions, we have to consider two other possible source terms. Due to the small value of N_{HI}, contributions to the local flux from low-density regions surrounding the galaxy, where photons from dark matter decay are not all absorbed locally, might be significant. We will refer to this as the "halo contribution." Furthermore, an additional contribution is given by the extragalactic UV photons created by the neutrino decay in the rest of the universe (here we neglect the effects of an additional quasar background flux). We evaluate the source function, ϕ as for $R/R_0 = 3$ in the expressions given by Sciama (1990) and we set $\epsilon = 1$ eV. In computing the interaction of the UV flux from radiative neutrino decay with H I at the edge of galaxies, we solve the radiative transfer equation through the slab taking into account the contribution of all three components to the local equilibrium. The external flux usually dominates in the upper layers but its exact contribution to the total flux in each point of the slab depends upon the external pressure and self gravity for Model A and on the dark matter density and velocity dispersion for Model B.

If the medium has a scale height as in Model B1 or B2, the volume density n is quite small and the medium is still fully ionized for column densities $N_{tot} \sim 10^{20}$ cm^{-2}. This is due to the large number of ionizing photons or equivalently to the inequality $n < \sqrt{\phi/\alpha_2}$. Until self-gravity sets in by compressing the gas vertically there is no neutral phase. Since for outer disks we are interested in models in which H I is present at the level of 5–8 $\times 10^{19}$ cm^{-2}, we ignore these highly ionized disks. We restrict our attention to cases with smaller scale height, i.e., a larger value of K/T^*, which require more flattened dark matter halos. This means that in order to obtain the edge at the correct column density, one needs smaller scale heights for Sciama models than for QSO background models, or equivalently slightly larger values of P_{ext} or of K/T^*. In Table 1 the last five entries show the results as we vary the galaxy parameters (two for Model A and three for Model B). Figures 4 and 5 show N_{HI} and N_{tot} versus x or R. Models AS2 and BS3 can again be excluded because of the small R_l and large χ^2. The other three Sciama models shown in Table 1 give quite good fits and realistic R_l-values. It is interesting that, when parameters are adjusted to give the same $N_{1/2}$, the predicted sharpness of the edge is similar for Model A and Model B and it does not differ appreciably from what we get using the Madau flux instead of the decaying neutrinos flux.

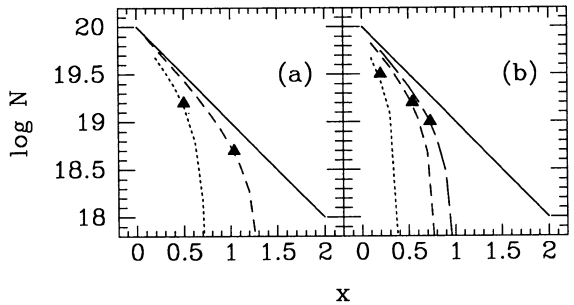

FIG. 4.—Same as in Fig. 1, we plot N_{tot} (*solid line*) and N_{HI} (*dashed lines*) as functions of the dimensionless x. Here we used a flux as given by the neutrino decay (inside and outside the slab) at 3 solar radii. Filled triangles indicate the H I column density at $N_{tot} = N_{1/2}$. In (*a*) we plot the H I column density for Case AS1 (*small dashed line*) and AS2 (*medium dashed line*) as given in Table 1. In (*b*) we plot the H I column density for Case BS1 (*small dashed line*), BS2 (*medium dashed line*), and BS3 (*large dashed line*).

6. SUMMARY AND DISCUSSION

In this paper and in Paper I we have discussed two type of H I observations which can be used to constrain the spectrum of the ionizing radiation below 1 keV. Observations show that neutral hydrogen in outer regions of spiral galaxies is warm and in Paper I we have calculated the heat input required from ionizing or nonionizing sources. We have shown that the ionizations from background photons, together with collisions due to self-gravity, are sufficient to bring the spin temperature well above 2.7 K even if there are no photons below 0.5 keV. This means that N_{HI} does not differ appreciably from the value

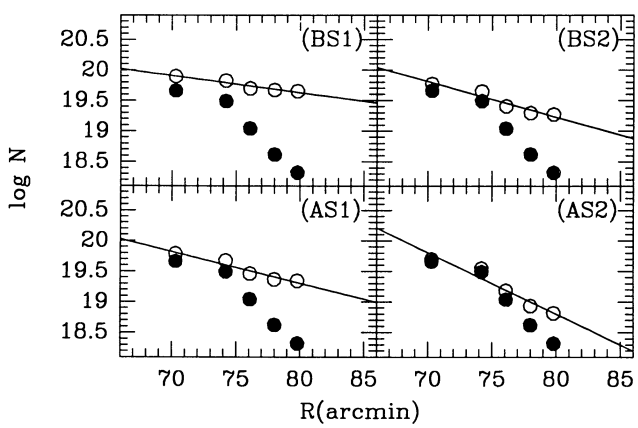

FIG. 5.—Values of N_{HI} observed near the edge in M33 (*filled circles*) and the corresponding total gas density N_{tot} (*open circles*) for four decaying neutrinos models described in Table 1.

N_B, inferred from the 21 cm brightness temperature. Therefore H I edges observed in the brightness column density of outer disks before it reaches 2×10^{19} cm^{-2} (Corbelli et al. 1989; van Gorkom 1991) correspond to real cutoffs in the neutral phase of the hydrogen distribution.

In order to get a sharp H I edge the intensity of the background flux needs to be stronger than the extrapolation at low energies of the power law observed above 2 keV. In this paper we have modeled the extragalactic ionizing UV flux by means of an intensity parameter I and a spectral index s (eq. [1]). We have used two alternative, simplified, models to determine the distributions of the gas pressure P and the volume density n as function of height z above the plane. They have effectively only one free parameter each. In Model A we assume that P and n are connected by the ideal gas law, involving the microscopic gas kinetic temperature T_K; we do not consider dark matter gravity explicitly and use a compression term P_{ext} as a free parameter. In this model when the gas column density is high enough, the cold H I phase forms near the Galactic plane with much larger n and smaller thickness than the warm H I and H II (for this thin slab, dark matter gravity is indeed unimportant). In Model B we introduce a dark matter gravity term, K, and assume that the density stratification is that of an isothermal slab which has some macroscopic temperature T^*. In the range of column densities we are interested in, results depend mostly on the single free parameter K/T^*. Model B is appropriate if outer disks are fairly homogeneous with weak contrast between cloud structure and diffuse medium. Magnetic pressure, cosmic-ray pressure, or turbulence allow T^* to be larger than T_K. The cold H I phase which occurs just inside the edge has higher kinetic temperatures and larger scale heights than for Model A. We assume that P_{ext} (for Model A) and K/T^* (for Model B) are constant across the radial interval where the H I edge occurs and we compute $N_{H\,I}$ as a function of N_{tot} for different background spectra.

The ranges of spectral indices and flux densities of the ionizing background radiation compatible with H I edges observations are also compatible with Hα measurements and evolutionary studies of the background ionizing flux. The spectral shape is in principle important; in practice we find the somewhat surprising but simple result that for any spectral index $s \gtrsim 1.4$ results depend rather weakly on the spectral shape. What is more important is the intensity of the flux at energies close to 13.6 eV which determines the ionization rate per neutral hydrogen atom, ζ, or the parameter $N_{1/2}$, defined as the value of N_{tot} where $N_{H\,I} = N_{H\,II}$ and roughly proportional to ζ/n. Spectra and models which give similar values of $N_{1/2}$ predict similar sharp edges. We have shown that Model A, Model B, or the decaying neutrino model can all give reasonable fits to the H I edge observed in M33 if their free parameter is such that $N_{1/2} > 2 \times 10^{19}$ cm^{-2}. If the extragalactic flux just above the Lyman edge is close to what Madau predicts ($s \sim 2.5$, $I \sim 1.4$), $N_{1/2} > 2 \times 10^{19}$ cm^{-2} implies $P_{ext} \ll 50$ cm^{-3} K for Model A, or $z_{H\,I} \gtrsim 0.5$ kpc for Model B (as for an almost spherical dark matter halo). For a galaxy with a modest inclination respect to our line of sight as $N_{1/2}$ gets larger the fits improve.

As P_{ext} or K/T^* decreases, the transition column density, $N_{1/2}$, and the sharpness of the edge increases. In the case of a quasar background, the number of ionizing photons coming from distant extragalactic sources is likely to be constant. Galaxies with a higher pressure, i.e., with a substantial amount of coronal gas or dark matter in outer regions, should then present a smaller value of $N_{1/2}$ and smoother edges. Similarly, H I column densities smaller than $N_{1/2}$ can survive in HVC if they have a vertical scale height smaller than that of outer disks due to stronger compression (from P_{ext} or local dark matter). With the observational sensitivity available at the moment, this may have led to a selection bias: edges which occur at larger H I column densities are easier to observe, and the observed sharpness may then be larger than the average. The galaxy NGC 3198 shows an H I edge rather similar to that of M33. This is not too surprising since they might have similar dark matter densities (for spherical halos $V/R \sim 5$–6 km s^{-1} kpc^{-1} for both galaxies). However, if the dark matter density changes from one type of galaxy to another, then we expect corresponding changes in the H I edge.

If decaying neutrinos provide the UV ionizing photons then the H I scale height must be quite small ($z_{H\,I} < 0.5$ kpc) for the gas to stay mostly neutral at $N_{tot} \sim 10^{20}$ cm^{-2}. However, once this small scale height is provided, by using for example a flat dark matter halo or a low T^*, the sharpness of the H I edge is rather similar to that predicted by a quasar background flux which gives the same $N_{1/2}$ value. For the outer disk for our Galaxy $z_{H\,I} > 0.5$ kpc, however, there are no observations of the H I vertical scale height just inside a sharp H I edge. These observations would be of great interest for selecting the most appropriate model (decaying neutrons, Model A or Model B) for outer disks with a sharp H I edge. We hope that in the near future detailed observations of other H I edges will become available together with measurements of the H I spin temperature and gas vertical scale height just before the edge occurs.

We are grateful to J. Charlton, P. Lenzuni, R. Reynolds, M. Roberts, D. Sciama, J. H. van Gorkom, and to the referee for useful comments to the original manuscript. This work was supported in part by NSF grant AST 91-19475, INT 89-13558, and by Agenzia Spaziale Italiana.

REFERENCES

Bajtlik, S., Duncan, R. C., & Ostriker, J. P. 1988, ApJ, 327, 570
Bochkarev, N. G., & Sunyaev, R. A. 1977, Soviet Astron., 21, 542
Charlton, J. C., Salpeter, E. E., & Hogan, C. J. 1993, ApJ, 402, 493
Colgan, S. W. J., Salpeter, E. E., & Terzian, Y. 1990, ApJ, 351, 503
Corbelli, E., & Salpeter, E. E. 1988, ApJ, 326, 551
———. 1993, ApJ, 419, 94 (Paper I)
Corbelli, E., Schneider, S. E., & Salpeter, E. E. 1989, AJ, 97, 390
Dickey, J. M., Hanson, M. M., & Helou, G. 1990, ApJ, 352, 522
Felten, J. E., & Bergeron, J. 1969, Astrophys. Lett., 4, 155
Huchtmeier, W. K., & Bohnenstengel, H. D. 1981, A&A, 100, 72
Ibañez, S. M. H., & di Sigalotti, L. 1984, ApJ, 285, 784
Ikeuchi, S., & Turner, E. L. 1991, ApJ, 381, L1
Kulkarni, S. R., Blitz, L., & Heiles, C. 1982, ApJ, 259, L63
Kulkarni, S. R., & Heiles, C. 1988, in Galactic and Extragalactic Radio Astronomy, ed. G. L. Verschuur & K. I. Kellerman (New York: Springer), 95
Kutyrev, A. S., & Reynolds, R. J. 1989, ApJ, 344, L9
Madau, P. 1992, ApJ, 389, L1
Maloney, P. 1993, ApJ, 414, 41
Melott, A. L. 1994, Soviet Astron., 28, 478
Merrifield, M. R. 1992, AJ, 103, 1552
Sargent, W. L. W., Young, P. J., Boksenberg, A., Carswell, R. F., & Whelan, J. A. J. 1979, ApJ, 230, 49
Sciama, D. W. 1990, ApJ, 364, 549
———. 1991, A&A, 245, 243
Shostak, G. S., & van der Kruit, P. C. 1984, A&A, 132, 20
Silk, J., & Sunyaev, R. A. 1976, Nature, 260, 508
Songalia, A., Bryant, W., & Cowie, L. L. 1989, ApJ, 345, L71
Spitzer, L. 1942, ApJ, 95, 329
———. 1978, Physical Processes in The Interstellar Medium (New York: Wiley)
Sunyaev, R. A. 1969, Astrophys. Lett., 3, 33
van Gorkom, J. H. 1991, in Proc. 3d Haystack Obs. Conf. on Atoms, Ions, and Molecules, ed. A. D. Haschick & P. T. P. Ho (ASP Conf. Ser., 16), 1